New Waveguide Structures for Millimeter-Wave and Optical Integrated Circuits

WILLIAM V. McLEVIGE, STUDENT MEMBER, IEEE, TATSUO ITOH, SENIOR MEMBER, IEEE, AND RAJ MITTRA, FELLOW, IEEE

Abstract—**Some new dielectric waveguide structures suitable for millimeter-wave and optical integrated circuits are presented. A method of analyzing wave propagation in these guides is developed by assuming simple field distribution and approximating the various regions of the guides in terms of effective dielectric constants. The mathematical formulation utilized results in simple eigenvalue equations from which the dispersion characteristics of the waveguides are readily obtained. Experimental results are described and the agreement between theory and experiment is shown to be quite good.**

I. INTRODUCTION

IN RECENT YEARS much research has been directed towards the use of millimeter- and submillimeter-wave frequencies for the transmission of information. As conventional metal waveguides become quite lossy and more difficult to fabricate as the wavelengths involved become shorter, alternative waveguiding structures made from dielectric materials have been proposed. Dielectric rectangular guides for millimeter-wave and optical frequencies have been described by a number of authors [1]–[5].

In this paper three new types of waveguide structures are presented, and a method of obtaining their theoretical dispersion characteristics and field distributions is developed. Fig. 1 depicts the coupled-line cross sections of these guides. The same analytical technique is easily extended to the single-line case of each waveguide.

The strip dielectric guide [Fig. 1(a)] and the insulated image guide [Fig. 1(b)] both utilize a conducting ground plane which may be used for heat sinking and/or dc biasing circuits. Thus these types of guides are especially well suited for millimeter-wave integrated circuits involving active devices requiring dc power [6], [7].

In dielectric waveguides most of the energy is confined to propagate in the region having the highest dielectric constant. In the strip dielectric guide [Fig. 1(a)] this confinement of energy occurs in the dielectric layer which is most easily and accurately fabricated, thus minimizing radiation losses due to mechanical irregularities on the side walls. On the other hand, the insulated image guide [Fig. 1(b)] has the advantage that most of the energy travels in the upper dielectric rod away from the conducting ground plane and its associated losses.[1] The strip-slab guide [Fig. 1(c)] does not have a ground plane as it is designed for use in optical integrated circuits.

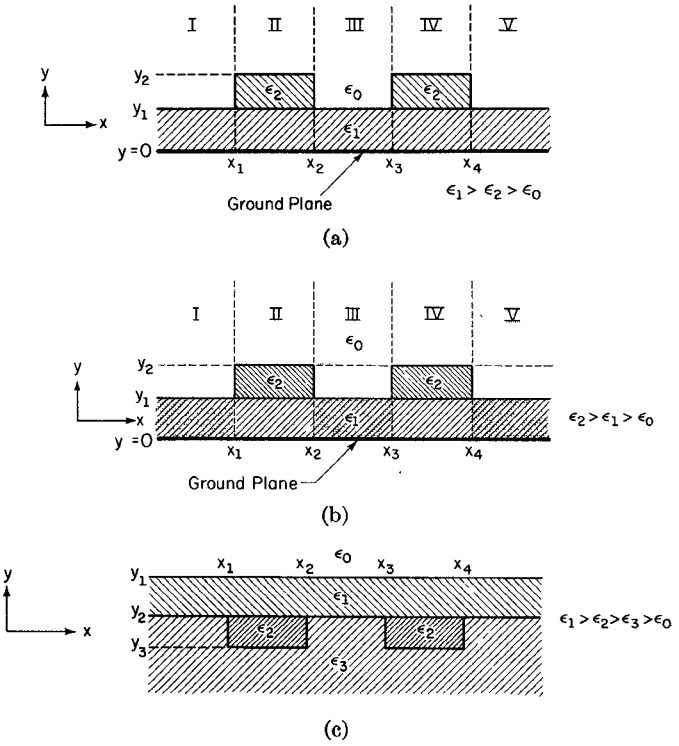

Fig. 1. Coupled dielectric-waveguide cross sections. (a) Strip dielectric guide. (b) Insulated image guide. (c) Strip-slab guide.

II. METHOD OF ANALYSIS

Dielectric rectangular waveguides will support the propagation of waves having two possible field configurations, classified as the E_{pq}^{y} and E_{pq}^{x} modes [8], where the subscripts p and q indicate the number of extrema of the electric field in the y and x directions, respectively. These modes are commonly referred to as being hybrid in nature because they do not possess the simpler field distributions of either the transverse magnetic (TM) or the transverse electric (TE) modes common to metal

Manuscript received February 20, 1975; revised April 25, 1975. This work was supported in part by Joint Services Electronics Program DAABC-0259, and in part by U. S. Army Research Grant DAHC04-74-G0113.

The authors are with the Department of Electrical Engineering and the Coordinated Science Laboratory, University of Illinois at Urbana-Champaign, Urbana, Ill. 61801.

[1] For the strip dielectric guide, conductor losses may be reduced by inserting another dielectric layer between the guiding layer and the ground plane and choosing its dielectric constant smaller than that of the guiding layer.

rectangular waveguides. We can, however, express the solution of Maxwell's equations for the rectangular guide in terms of two scalar potentials, ϕ^e and ϕ^h. The field components become [9]

$$E_x = \frac{1}{\epsilon_r(y)} \frac{\partial^2 \phi^e}{\partial y \partial x} + \omega \mu k_z \phi^h \tag{1}$$

$$E_y = \frac{1}{\epsilon_r(y)} \left(k_z^2 - \frac{\partial^2}{\partial x^2} \right) \phi^e \tag{2}$$

$$E_z = \frac{-jk_z}{\epsilon_r(y)} \frac{\partial \phi^e}{\partial y} - j\omega\mu \frac{\partial \phi^h}{\partial x} \tag{3}$$

$$H_x = -\omega \epsilon k_z \phi^e + \frac{\partial^2 \phi^h}{\partial y \partial x} \tag{4}$$

$$H_y = \left(k_z^2 - \frac{\partial^2}{\partial x^2} \right) \phi^h \tag{5}$$

$$H_z = j\omega\epsilon \frac{\partial \phi^e}{\partial x} - jk_z \frac{\partial \phi^h}{\partial y} \tag{6}$$

where ϵ and μ are the permittivity and permeability of free space, $\epsilon_r(y)$ is a relative dielectric constant in the region of application, and k_z is the propagation constant in the z direction.

Since the E_{pq}^y modes have principal E- and H-field components in the y and x directions, respectively, ϕ^e has the dominant contribution to the modal field. Similarly, for the E_{pq}^x modes, the principal field components are E_x and H_y, and ϕ^h has the dominant contribution to the modal field. Hence we can set $\phi^h = 0$ in (1) through (6) and write the solution for the E_{pq}^y modes, or set $\phi^e = 0$ and write the solution for the E_{pq}^x modes. Since both sets of modes are similar, we will concern ourselves here with only the E_{pq}^y modes. The solution for the propagation constant k_z found in this manner will be quite close to the solution obtained using the more rigorous approach of using both ϕ^h and ϕ^e in the field expressions.

III. FORMULATION OF THE BOUNDARY VALUE PROBLEM

In our analysis we extend the method of effective dielectric constants originally developed by Knox and Toulios for the image guide [3] and the "insular guide" (insulated image guide) [7]. The analytical approach is essentially the same for all three types of guide structures studied. The mathematical formulation will be presented in depth for only the strip dielectric guide. The significant differences in the analysis of the other two types of guides will be pointed out later. In the case of insulated image guides, the analysis actually coincides with that reported in [7]. In all cases we will assume the dielectric materials and conductor to be lossless.

A rigorous solution of Maxwell's equations for the strip dielectric guide structure [Fig. 1(a)] would be exceedingly complex. However, it is possible to introduce a simplification by the use of the concept of effective dielectric constants. If regions I, II, III, IV, and V in Fig. 1(a) are taken to be infinitely long in the x direction, we have five multilayered slab waveguides. Regions I, III, and V will then have the cross section depicted in Fig. 2(a), while the cross sections of regions II and IV will become that of Fig. 2(b). The propagation constants for these single- and double-slab waveguides can be determined by matching the tangential electric and magnetic fields across each boundary. Both of these structures consisting of one or two dielectric slabs with a conducting ground plane on one side and air on the other can be equivalently replaced by an infinite homogeneous region having some effective dielectric constant defined analytically later in our analysis. The effective dielectric constant may be interpreted as that of a hypothetical medium in which the propagation constant is identical to that of the original structure.

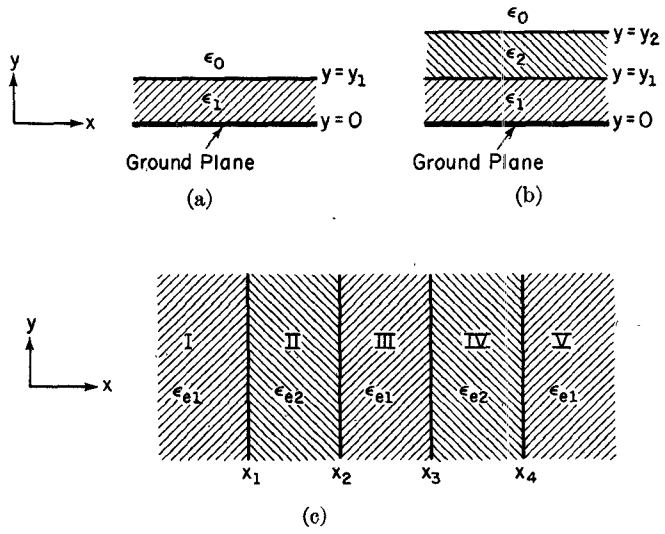

Fig. 2. Three steps in dielectric-waveguide analysis. (a) Structure for analyzing y variation in single-layered regions. (b) Structure for analyzing y variation in double-layered regions. (c) Structure for analyzing x variation using concept of effective dielectric constant.

Having determined the effective dielectric constants of the various regions, the guide in Fig. 1(a) can then be analyzed by modeling it with the five-layered structure shown in Fig. 2(c), where ϵ_{e1} is the effective dielectric constant of the single-slab guide and ϵ_{e2} is the effective dielectric constant of the double-slab guide. The propagation constant k_z for the original guide is determined by matching the tangential fields on the boundaries in Fig. 2(c). The individual steps in this method of analysis will now be discussed in greater detail.

IV. DERIVATION OF THE EIGENVALUE EQUATIONS

We first derive the eigenvalue equation describing wave propagation in the double-layered dielectric slab shown in Fig. 2(b), which corresponds to regions II and IV in Fig. 1(a). Noting that for the E_{pq}^y modes $\phi^h = 0$, we

see from (1)–(6) that the tangential fields we are interested in matching in Fig. 2(b) are the H_x and E_z components. The relationships between these components and ϕ_e are

$$H_x \sim \phi^e \tag{7}$$

$$E_z \sim \frac{1}{\epsilon_r(y)} \frac{\partial \phi^e}{\partial y}. \tag{8}$$

For the structure in Fig. 2(b), we know most of the power will travel inside the slab having the highest dielectric constant. We therefore write the field distribution ϕ^e as sinusoidally varying in the y direction in the ϵ_1 region. In the ϵ_2 region we allow for the possibility of the field being either sinusoidal or exponentially decaying by expressing it in terms of a sum of hyperbolic functions. Outside the guide in the ϵ_0 region the field will exponentially decay in the y direction. The presence of the conducting ground plane at $y = 0$ forces the tangential electric field to be zero there. Since the guide is assumed to be infinitely wide, there is no x variation in the fields. We therefore write the fields as

$$\phi^e(y) = A \cos k_y y, \qquad 0 \leq y \leq y_1 \tag{9}$$

$$\phi^e(y) = B^c \cosh [\eta_2(y - y_1)] + B^s \sinh [\eta_2(y - y_1)], \qquad y_1 \leq y \leq y_2 \tag{10}$$

$$\phi^e(y) = C \exp [-\eta_0(y - y_2)], \qquad y_2 \leq y \tag{11}$$

where η_0 and η_2 are attenuation constants in their respective regions and subject to the relation

$$k_{zs2}^2 = \epsilon_1 k_0^2 - k_y^2 = \epsilon_2 k_0^2 + \eta_2^2 = \epsilon_0 k_0^2 + \eta_0^2 \tag{12}$$

where η_0 must be real and greater than zero to ensure the field will diminish for large y, and η_2 may be either real or imaginary. In (12) k_0 represents the free-space wavenumber; ϵ_0, ϵ_1, and ϵ_2 are the relative dielectric constants of their respective regions (ϵ_0 is unity in air); and k_{zs2} is the propagation constant of the double-slab waveguide in Fig. 2(b).

Matching the field components H_x and E_z at $y = y_1$, we obtain

$$A \cos k_y y_1 = B^c \tag{13}$$

$$\frac{-A k_y \sin k_y y_1}{\epsilon_1} = \frac{B^s \eta_2}{\epsilon_2} \tag{14}$$

and similarly at $y = y_2$

$$B^c \cosh [\eta_2(y_2 - y_1)] + B^s \sinh [\eta_2(y_2 - y_1)] = C \tag{15}$$

$$\frac{\eta_2}{\epsilon_2} \{B^c \sinh [\eta_2(y_2 - y_1)] + B^s \cosh [\eta_2(y_2 - y_1)]\} = \frac{-\eta_0}{\epsilon_0} C. \tag{16}$$

The four equations (13)–(16) can be algebraically manipulated to eliminate the four constants A, B^c, B^s, and C, leaving the eigenvalue equation for k_y

$$k_y \sin k_y y_1 \left\{ \frac{\eta_0 \epsilon_2^2}{\eta_2} \sinh [\eta_2(y_2 - y_1)] + \epsilon_2 \epsilon_0 \cosh [\eta_2(y_2 - y_1)] \right\} - \epsilon_1 \cos k_y y_1 \{\epsilon_0 \eta_2 \sinh [\eta_2(y_2 - y_1)] + \epsilon_2 \eta_0 \cosh [\eta_2(y_2 - y_1)]\} = 0. \tag{17}$$

The lowest value of k_y will produce the fundamental mode E_{p1}^y; the second lowest value of k_y will produce the E_{p2}^y modes, and so on, where the subscript p is the mode index in the x direction of the original structure and will be determined in a later step of our analysis. To positively identify what mode a particular solution corresponds to, it is best to look at the field distribution $\phi^e(y)$. This can be done by choosing one of the constants in (13)–(16) arbitrarily and solving for the others. The resulting expressions give the relative magnitude of the fields, from which the number of extrema of the electric field can be readily determined.

We may write (12) in the equivalent form

$$k_{zs2}^2 = \epsilon_{e2} k_0^2 \tag{18}$$

where

$$\epsilon_{e2} = \epsilon_1 - \frac{k_y^2}{k_0^2}. \tag{19}$$

The effective dielectric constant ϵ_{e2} will be used later in our analysis when we will model the layered structure of Fig. 2(b) with a single homogeneous region having a dielectric constant ϵ_{e2}.

Using the same procedure presented for the double-layered slab in Fig. 2(b), a second eigenvalue equation describing wave propagation in the single-layered slab shown in Fig. 2(a) is derived. This single slab corresponds to regions I, III, and V of Fig. 1(a). ϕ^e is again assumed to be sinusoidally varying in the ϵ_1 region and exponentially decaying outside the slab. Matching H_x and E_z on the boundary at $y = y_1$ gives the eigenvalue equation for $\bar{k}_y$

$$\bar{k}_y \epsilon_0 \sin \bar{k}_y y_1 - \eta \epsilon_1 \cos \bar{k}_y y_1 = 0. \tag{20}$$

We can express the attenuation constant η in terms of $\bar{k}_y$ by the relation

$$k_{zs1}^2 = \epsilon_1 k_0^2 - \bar{k}_y^2 = \epsilon_0 k_0^2 + \eta^2 \tag{21}$$

where k_{zs1} is the propagation constant of the single-slab waveguide in Fig. 2(a). The effective dielectric constant ϵ_{e1} for this structure is defined by

$$\epsilon_{e1} = \epsilon_1 - \frac{\bar{k}_y^2}{k_0^2}. \tag{22}$$

V. PROPAGATION CONSTANT OF THE STRIP DIELECTRIC GUIDE

We are now ready to analyze the five-layered vertical slab structure in Fig. 2(c), having determined the effective dielectric constants ϵ_{e1} and ϵ_{e2}. Since the slabs are infinite in the y direction, there is only an x variation in the

fields. Most of the energy travels in the two ϵ_{e2} regions (II and IV) where we will assume a sinusoidally varying field. The two outer regions (I and V) will have exponentially decaying fields, while the region III fields will be written as the sum of hyperbolic functions. The field expressions are, therefore,

$$\phi^e(x) = A_1 \exp[\xi(x - x_1)], \qquad x \leq x_1 \quad (23)$$

$$\phi^e(x) = B_1{}^c \cos[k_x(x - x_1)] + B_1{}^s \sin[k_x(x - x_1)], \qquad x_1 \leq x \leq x_2 \quad (24)$$

$$\phi^e(x) = C_1{}^c \cosh[\xi(x - x_2)] + C_1{}^s \sinh[\xi(x - x_2)], \qquad x_2 \leq x \leq x_3 \quad (25)$$

$$\phi^e(x) = D_1{}^c \cos[k_x(x - x_3)] + D_1{}^s \sin[k_x(x - x_3)], \qquad x_3 \leq x \leq x_4 \quad (26)$$

$$\phi^e(x) = E_1 \exp[-\xi(x - x_4)], \qquad x_4 \leq x \quad (27)$$

where k_x is the propagation constant in the x direction in the ϵ_{e2} regions and ξ is the attenuation constant in the ϵ_{e1} regions. The analogous equation to (12) and (21) is

$$k_z{}^2 = \epsilon_{e1}k_0{}^2 + \xi^2 = \epsilon_{e2}k_0{}^2 - k_x{}^2 \quad (28)$$

where k_z is the propagation constant of the five-layered structure in Fig. 2(c) and is assumed in the present analysis to be identical to that of the original structure, the strip dielectric guide.

The tangential fields we are interested in matching are the E_y and H_z. From (2) and (6) we note the following relations:

$$E_y \sim \phi^e \quad (29)$$

$$H_z \sim \frac{\partial \phi^e}{\partial x}. \quad (30)$$

By matching the fields at each dielectric interface and eliminating the constants, we obtain the eigenvalue equation for k_x

$$\{T_1\xi \cosh[\xi(x_3 - x_2)] - T_2k_x \sinh[\xi(x_3 - x_2)]\}T_4 - \{T_2k_x \cosh[\xi(x_3 - x_2)] - T_1\xi \sinh[\xi(x_3 - x_2)]\}T_3 = 0 \quad (31)$$

where

$$T_1 = \xi \sin[k_x(x_4 - x_3)] + k_x \cos[k_x(x_4 - x_3)]$$

$$T_2 = k_x \sin[k_x(x_4 - x_3)] - \xi \cos[k_x(x_4 - x_3)]$$

$$T_3 = \xi k_x \cos[k_x(x_2 - x_1)] + \xi^2 \sin[k_x(x_2 - x_1)]$$

$$T_4 = -k_x{}^2 \sin[k_x(x_2 - x_1)] + \xi k_x \cos[k_x(x_2 - x_1)].$$

After using the computer to solve for k_x, we can then use (28) and calculate k_z and, hence, the dispersion characteristics of the original waveguide.

Again we are confronted with the same uncertainty as to what mode a particular solution of (31) corresponds. The relative magnitude of the field distribution $\phi^e(x)$ can be determined as before by choosing one of the constants in (23)–(27) to be arbitrary and then solving for the others through use of the boundary conditions. The subscript p in the $E_{pq}{}^y$ modes is given by the number of extrema of $\phi^e(x)$.

The special case of the single line can be derived from the coupled-line analysis by letting the separation between guides go to infinity and taking the analytical limit. If we let $x_3 - x_2 \to \infty$, the eigenvalue equation (31) reduces to

$$(\xi^2 - k_x{}^2) \sin[k_x(x_2 - x_1)] + 2\xi k_x \cos[k_x(x_2 - x_1)] = 0. \quad (32)$$

VI. EXTENSION OF ANALYSIS TO THE INSULATED IMAGE GUIDE

Applying the same method of analysis to the insulated image guide [Fig. 1(b)] is straightforward. Since most of the energy will travel in the two higher dielectric-constant regions, we will neglect the fields in the shaded regions in Fig. 1(b). Hence the effective dielectric constant ϵ_{e1} in the single-layered regions (I, III, and V) is the same as that of free space (ϵ_0). Regions II and IV are again modeled by the double-slab guide in Fig. 2(b), and an effective dielectric constant ϵ_{e2} is determined. Fig. 2(c) is then utilized to analyze wave propagation in the original structure.

The field expressions $\phi^e(y)$ for the slab guide [Fig. 2(b)], corresponding to regions II and IV of Fig. 1(b), are somewhat different for the insulated image guide. Since most of the power travels in the ϵ_2 region, a sinusoidal field variation is assumed there. In the lower dielectric-constant ϵ_1 region, the possibility of the fields being either exponentially decaying or sinusoidally varying allows one to express $\phi^e(y)$ in terms of the hyperbolic cosine. Outside the guide the field decays exponentially.

Enforcing the continuity of H_x and E_z on the dielectric interfaces, we derive the eigenvalue equation for k_y

$$\eta_3\epsilon_2k_y\epsilon_1 \cosh \eta_1y_1 \cos[k_y(y_2 - y_1)] + \eta_3\epsilon_2{}^2\eta_1 \sinh \eta_1y_1 \sin[k_y(y_2 - y_1)] - \epsilon_0k_y{}^2\epsilon_1 \cosh \eta_1y_1 \sin[k_y(y_2 - y_1)] + \epsilon_0k_y\epsilon_2\eta_1 \sinh \eta_1y_1 \cos[k_y(y_2 - y_1)] = 0 \quad (33)$$

where η_1 and η_3 are attenuation constants subject to the relation

$$k_{zs3}{}^2 = \epsilon_0k_0{}^2 + \eta_3{}^2 = \epsilon_2k_0{}^2 - k_y{}^2 = \epsilon_1k_0{}^2 + \eta_1{}^2 \quad (34)$$

where k_{zs3} is the propagation constant for the double-slab guide [Fig. 2(b)] with $\epsilon_2 > \epsilon_1$. The effective dielectric constant ϵ_{e2} is given by

$$\epsilon_{e2} = \epsilon_2 - \frac{k_y{}^2}{k_0{}^2}. \quad (35)$$

The x variation in the fields is then modeled using Fig. 2(c), and the resulting eigenvalue equation (31) for k_x is identical to that of the strip dielectric guide. The propagation constant k_z of the original guide is likewise given by (28).

VII. STRIP-SLAB GUIDE

The preceding analysis is applicable to more exotic waveguides such as that in Fig. 1(c). This structure, which we shall refer to as the strip-slab guide, is designed for use in optical integrated circuits. If one uses the same analytical approach as before, regions II and IV in Fig. 1(c) are modeled by a four-layered slab guide with relative dielectric constants ϵ_0, ϵ_1, ϵ_2, and ϵ_3 for the various layers. A field sinusoidally varying in the y direction is assumed in the highest dielectric-constant (ϵ_1) region. In the ϵ_2 region $\phi^e(y)$ is written in terms of hyperbolic functions to allow the field to be either sinusoidal or exponentially decaying. Outside the guide and in the ϵ_3 substrate, the field decays exponentially. Matching the tangential fields on each boundary gives the eigenvalue equation for k_y

$$(\epsilon_0 k_y G_1 - \eta_0 \epsilon_1 G_2) \sin [k_y(y_1 - y_2)] - (\eta_0 \epsilon_1 G_1 + \epsilon_0 k_y G_2) \cos [k_y(y_1 - y_2)] = 0 \quad (36)$$

where

$$G_1 = k_y \epsilon_2 \left\{ \epsilon_3 \cosh [\eta_2(y_2 - y_3)] + \frac{\epsilon_2 \eta_3}{\eta_2} \sinh [\eta_2(y_2 - y_3)] \right\}$$

$$G_2 = \epsilon_1 \{ \eta_2 \epsilon_3 \sinh [\eta_2(y_2 - y_3)] + \epsilon_2 \eta_3 \cosh [\eta_2(y_2 - y_3)] \}.$$

In (36), η_0, η_2, and η_3 are attenuation constants related to the propagation constant k_{zs4} of the four-layered slab guide by

$$k_{zs4}^2 = \epsilon_0 k_0^2 + \eta_0^2 = \epsilon_1 k_0^2 - k_y^2 = \epsilon_2 k_0^2 + \eta_2^2 = \epsilon_3 k_0^2 + \eta_3^2. \quad (37)$$

The effective dielectric constant ϵ_{e2} of this slab guide is given by (19).

Regions I, III, and V are modeled by a three-layered slab guide having relative dielectric constants ϵ_0, ϵ_1, and ϵ_2. Field variations identical with those assumed in the same dielectric layers of regions II and IV are employed to derive the eigenvalue equation for $\bar{k}_y$

$$(\eta_0 \eta_3 \epsilon_1^2 - \epsilon_0 \epsilon_3 \bar{k}_y^2) \sin [\bar{k}_y(y_1 - y_2)] + (\epsilon_0 \epsilon_1 \eta_3 \bar{k}_y + \epsilon_1 \epsilon_3 \eta_0 \bar{k}_y) \cos [\bar{k}_y(y_1 - y_2)] = 0 \quad (38)$$

where η_0 and η_3 are attenuation constants related to $\bar{k}_y$ by an equation of the same form as (37). The effective dielectric constant ϵ_{e1} for this slab structure is given by (22).

Fig. 2(c) is again used as the equivalent slab guide for which the same eigenvalue equation (31) for k_x is derived. The propagation constant k_z for the strip-slab guide is likewise given by (28).

VIII. EXPERIMENTAL DATA AND COMPARISON WITH THEORY

Dispersion curves for both the strip dielectric and insulated image guide were obtained experimentally at X band because of better availability of components designed to operate at the lower frequencies and greater ease in fabricating dielectric waveguides with dimensions on the order of 1 cm. Only the single-line structures were investigated in the laboratory. A study of coupled transmission lines was done on the computer.

As is evident from Fig. 3, the agreement between experiment and theory is excellent for the strip dielectric guide. The agreement between theory and experiment is found to be more sensitive to the geometry of the structure for the insulated image guide. Increasing the horizontal width and thus the aspect ratio while holding the other dimensions constant produced closer agreement between theory and experiment (Fig. 4). However, for the insulated image guides with smaller aspect ratio, theoretical curves start deviating from experimental data, although these results are not presented in graphical forms in this paper. This sensitivity to the geometry of the guide involved is due to the assumption in the analysis that each of the various regions of the guide can be approximated by a homogeneous medium having a certain effective dielectric constant and whose propagation constant is the same as that of an infinitely wide slab guide. Obviously, the narrower the various regions of the waveguide, or the greater the

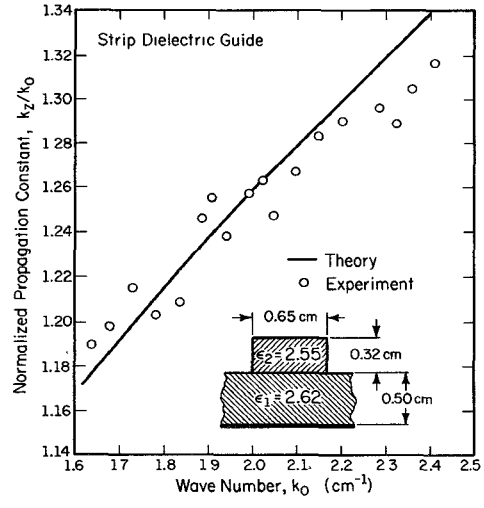

Fig. 3. Dispersion characteristics of the strip dielectric guide.

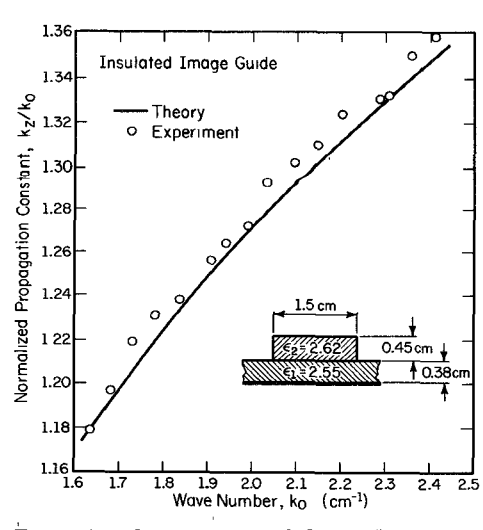

Fig. 4. Dispersion characteristics of the insulated image guide.

difference between the relative dielectric constants ϵ_2 and ϵ_1, the less accurate this method becomes. The agreement between theory and experiment tends to be better for the strip dielectric guide than for the insulated image guide because the effective dielectric constants for the various regions are closer in value for the strip dielectric guide. The effective dielectric constant of the single-slab regions of the insulated image guide is always taken to be that of free space since the fields inside the slab are neglected in that portion of the analysis.

Studies of the electric field strength as a function of the distance from the side wall of the double-layered region were also undertaken. Theoretical field plots are derived by solving for the constants in the equations for $\phi^e(x)$. Comparison with experimental data for the strip dielectric guide and the insulated image guide is good, as shown in Fig. 5(a) and (b).

Some numerical data for the dispersion characteristics are shown in Figs. 6–8 for both single and coupled versions of strip dielectric, insulated image, and strip-slab guides. It should be noted that for coupled-guide cases [Figs. 6(b), 7(b), and 8(b)] a slightly different notation has been used for the even and odd modes referred to in the literature. In our notation, E_{11}^y represents the dominant even mode, while E_{21}^y represents the dominant odd mode.

It should also be mentioned that for coupled line cases numerical difficulties have been occasionally encountered when a particular mode is approaching its cutoff. One source of difficulty occurs when the interval of allowed solutions does not include its end point. If an actual solution occurs very close to the end point of the interval, the accuracy of the solution may be limited by the number of significant figures the computer can handle. Another source of difficulty in searching for zeros of an equation within an interval using the bisection method is that the process can require a prohibitively long time because the interval taken must be small enough so that the function of

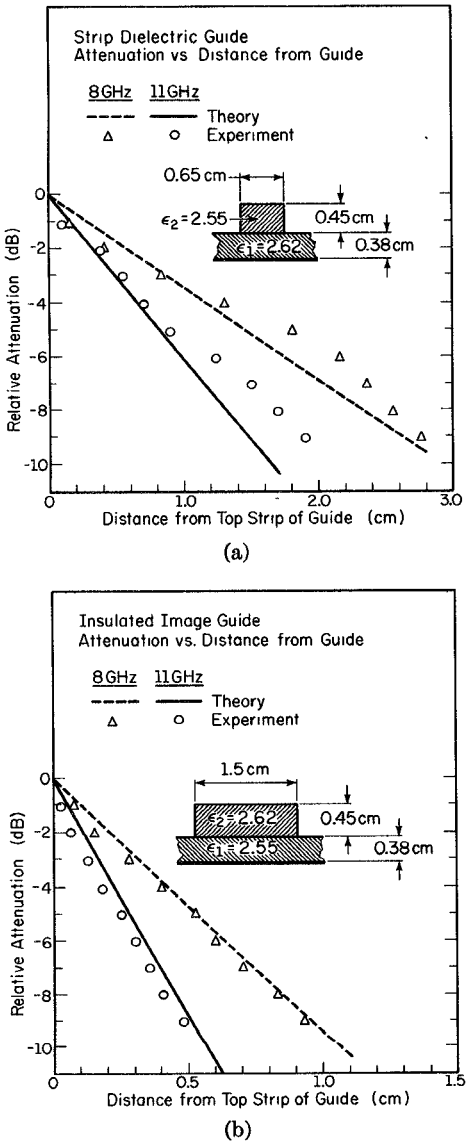

Fig. 5. Electric field strength as a function of the horizontal distance from the side wall of the double-layered region. (a) Strip dielectric guide. (b) Insulated image guide.

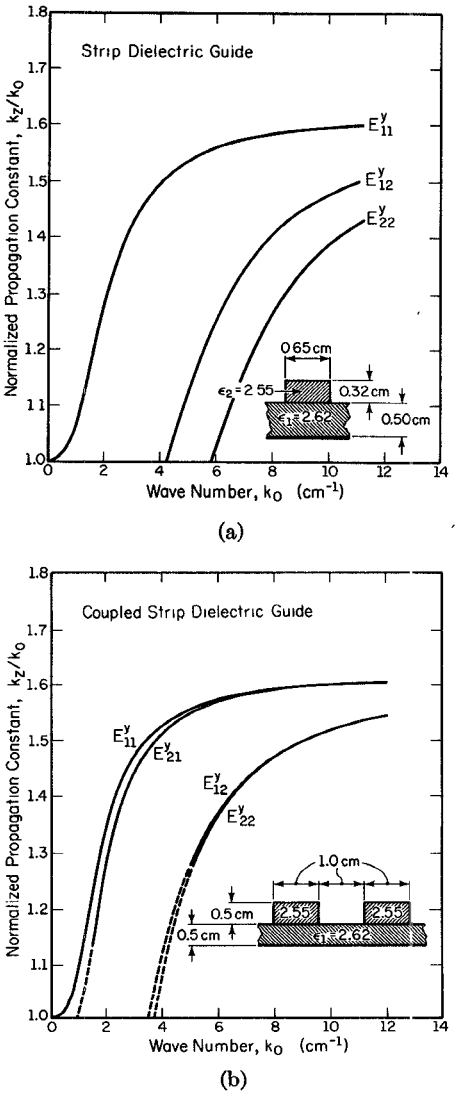

Fig. 6. Numerical data for the dispersion characteristics of a number of modes in the strip dielectric guide. (a) Isolated guide. (b) Coupled guide.

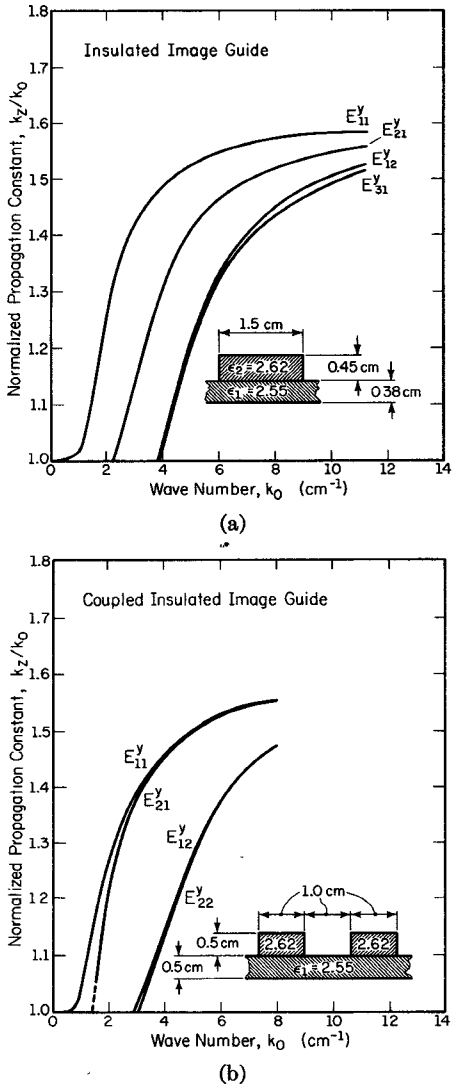

Fig. 7. Numerical data for the dispersion characteristics of a number of modes in the insulated image guide. (a) Isolated guide. (b) Coupled guide.

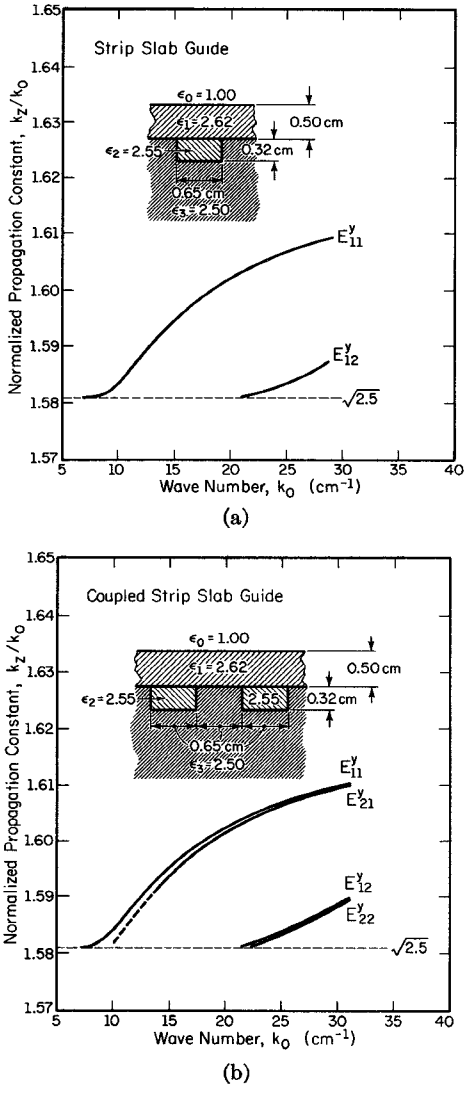

Fig. 8. Numerical data for the dispersion characteristics of a number of modes in the strip-slab guide. (a) Isolated guide. (b) Coupled guide.

interest will change its sign only once. The dashed lines on the theoretical dispersion curves are due to these kinds of numerical problems.

IX. CONCLUSIONS

We have shown the method of analysis, based on the concept of effective dielectric constant, to be an excellent approach to the study of certain types of dielectric waveguides. However, this approach is only an approximate technique, and can be expected to work well only for larger aspect ratios and when the difference between the relative dielectric constants involved is small.[2]

The strip dielectric guide and the insulated image guide are well suited for millimeter-wave circuit integration. Their simplicity in fabrication and lower material cost give them the edge over the conventional metal waveguide. The efficiency of dielectric guides as transmission lines may still remain a problem; loss calculations and further experimental work at millimeter-wave frequencies such as those reported in [7] are necessary.

[2] Knox and Toulios reported that in their experiments the concept of effective dielectric constant works well for the insular guide with any aspect ratio and relative dielectric-constant ratio [3].

REFERENCES

[1] E. A. J. Marcatili, "Dielectric rectangular waveguide and directional coupler for integrated optics," *Bell Syst. Tech. J.*, vol. 48, pp. 2079–2102, Sept. 1969.
[2] J. E. Goell, "A circular-harmonic computer analysis of rectangular dielectric waveguides," *Bell Syst. Tech. J.*, vol. 48, pp. 2133–2160, Sept. 1969.
[3] R. M. Knox and P. P. Toulios, "Integrated circuits for the millimeter through optical frequency range," in *Proc. Symp. Submillimeter Waves* (New York), Mar. 31–Apr. 2, 1970.
[4] P. P. Toulios and R. M. Knox, "Rectangular dielectric image lines for millimeter integrated circuits," presented at the Western Elec. Show and Conv., Los Angeles, Calif., Aug. 25–28, 1970.
[5] H. Jacobs and M. M. Chrepta, "Electronic phase shifter for millimeter-wave semiconductor dielectric integrated circuits," *IEEE Trans. Microwave Theory Tech.*, vol. MTT-22, pp. 411–417, Apr. 1974.
[6] R. M. Knox and P. P. Toulios, "A *V*-band receiver using image line integrated circuits," in *Proc. Nat. Electronics Conf.*, Oct. 16–18, 1974, pp. 489–492, Paper V29.
[7] P. P. Toulios and R. M. Knox, "Image line integrated circuits for system applications at millimeter wavelengths," Final Rep., Contract DAAB07-73-C-0217, U. S. Army Electronics Command Rep. ECOM-73-0217-F, July 1974.
[8] D. Marcuse, *Theory of Dielectric Optical Waveguides*. New York: Academic, 1974.
[9] R. F. Harrington, *Time-Harmonic Electromagnetic Fields*. New York: McGraw-Hill, 1961.